

Magnetic-Field-Induced Sign Changes of Thermal Expansion in DyCrO₄

Jin-Cheng He(何金城)^{1,2†}, Zhao Pan(潘昭)^{1,2†}, Dan Su(苏丹)^{1,2}, Xu-Dong Shen(申旭东)^{1,2},
Jie Zhang(张杰)^{1,2}, Da-Biao Lu(卢达标)^{1,2}, Hao-Ting Zhao(赵浩婷)^{1,2}, Jun-Zhuang Cong(丛君状)¹,
En-Ke Liu(刘恩克)^{1,2}, You-Wen Long(龙有文)^{1,2,3*}, and Young Sun(孙阳)^{1,4*}

¹Beijing National Laboratory for Condensed Matter Physics, Institute of Physics,
Chinese Academy of Sciences, Beijing 100190, China

²School of Physical Sciences, University of Chinese Academy of Sciences, Beijing 100190, China

³Songshan Lake Materials Laboratory, Dongguan 523808, China

⁴Center of Quantum Materials and Devices, and Department of Applied Physics,
Chongqing University, Chongqing 401331, China

(Received 11 April 2023; accepted manuscript online 15 May 2023)

The anharmonicity of lattice vibration is mainly responsible for the coefficient of thermal expansion (CTE) of materials. External stimuli, such as magnetic and electric fields, thus cannot effectively change the CTE, much less the sign variation from positive to negative or vice versa. In this study, we report significant magnetic field effects on the CTE of zircon- and scheelite-type DyCrO₄ prepared at ambient and high pressures, respectively. At zero field, the zircon-type DyCrO₄ exhibits a negative CTE below the ferromagnetic-order temperature of 23 K. With increasing field up to ≥ 1.0 T, however, the sign of the CTE changes from negative to positive. In the scheelite phase, magnetic field can change the initially positive CTE to be negative with a field up to 2.0 T, and then a reentrant positive CTE is induced by enhanced fields ≥ 3.5 T. Both zircon and scheelite phases exhibit considerable magnetostrictive effects with the absolute values as high as ~ 800 ppm at 2 K and 10 T. The strong spin–lattice coupling is discussed to understand the unprecedented sign changes of the CTE caused by applying magnetic fields. The current DyCrO₄ provides the first example of field-induced sign change of thermal expansion, opening up a way to readily control the thermal expansion beyond the conventional chemical substitution.

DOI: 10.1088/0256-307X/40/6/066501

Thermal expansion is an important physical performance parameter for material practical applications. A mismatch in coefficients of thermal expansion (CTEs) between different components in functional materials and devices could trigger a series of serious problems, leading to functional failure, deformation, and/or even cracks.^[1,2] In theory, thermal expansion is dominated by the anharmonicity of atomic vibration.^[3] Therefore, chemical substitution is often used to tune the magnitude of the CTE in a moderate temperature region. In particular, negative thermal expansion materials, in which the cell volumes contract instead of expanding upon heating, are frequently used to control the CTE by forming composites with normal positive-thermal-expansion materials. For example, effectively controlled thermal expansion from strong negative thermal expansion to near-zero thermal expansion was realized in La-doped PbTiO₃–BiFeO₃.^[4] In past decades, certain types of negative thermal expansion materials have been discovered, mainly including phonon-related frameworks,^[5–7] the magneto-volume effect in antiperovskites and alloys,^[8–10] metal–insulator transition in Ca₂RuO₄,^[11] charge transfer in LaCu₃Fe₄O₁₂,^[12] BiNiO₃,^[13] and SmS,^[14] and ferroelectrostriction in PbTiO₃-based ferroelectrics.^[15–17] As chemical modulation of the CTE is limited for most ma-

terials, a more effective and readily tunable method to modify the CTE of materials is urgently required.

Compared to chemical substitution, external fields like magnetic and electric fields are more desirable for tuning the CTE via peculiar physical effects such as magnetostrictive and ferroelectrostrictive effects. In fact, the magnitudes of CTEs in some magnetic materials can be changed by applying magnetic fields.^[18,19] However, there is no report, to date, of field-induced sign changes of the CTE from positive to negative or vice versa. In this Letter, we report a rare-earth chromate of DyCrO₄, in which the crystal structure depends on the synthesis conditions: a standard solid-state annealing method at ambient pressure produces a zircon-type (z-type) phase with space group $I4_1/amd$, whereas a high-pressure annealing method drives the structure to assume a scheelite-type (s-type) phase with space group $I4_1/a$. Intriguingly, the CTEs of both phases experience sign changes under external magnetic fields. Specifically, a field-induced negative-to-positive thermal expansion is found to occur in the z-type DyCrO₄, whereas positive-to-negative and then reentrant positive thermal expansions are observed in the s-type DyCrO₄. Field-induced sign changes of the CTE are thus realized for the first time in the current DyCrO₄ in its two polymorphs.

[†]These authors contributed equally to this work.

*Corresponding authors. Email: ywlong@iphy.ac.cn; youngsun@cqu.edu.cn

© 2023 Chinese Physical Society and IOP Publishing Ltd

Results and Discussion. As shown in Fig. 1, the Rietveld refinement analysis for the x-ray diffraction (XRD) patterns confirms that the ambient-pressure-synthesized DyCrO₄ crystallizes into a tetragonal z-type crystal structure with space group *I*4₁/*amd* [Figs. 1(a) and 1(c)], whereas the high-pressure-treated one possesses another tetragonal s-type structure in *I*4₁/*a* symmetry at room temperature [Figs. 1(b) and 1(d)], in good agreement with the literature.^[20–22] Details of the Rietveld refinements and related structural parameters were provided in the Supplementary Material (Table S1). The structural rearrangement causes a large volume reduction by ~10.9% per chemical formula, suggesting that the zircon-to-scheelite transition is of first order in nature.^[23] Correspondingly, the Dy–O–Cr bonding changes sharply, giving rise to essentially different magnetic properties for these two phases as shown below.

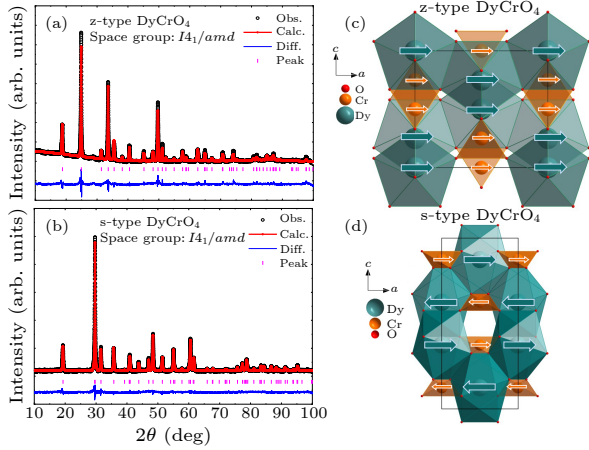


Fig. 1. Rietveld refinement of x-ray powder diffraction patterns of (a) z-type DyCrO₄ (Cu *K*_α) and (b) s-type DyCrO₄ at room temperature. (c) The zircon-type and (d) scheelite-type crystal structures of DyCrO₄. Directions of spin moments are indicated by arrows.

Figure 2(a) displays the temperature dependence of magnetic susceptibility for the z-type DyCrO₄. As reported previously, a paramagnetic (PM) to ferromagnetic (FM) phase transition is found to occur with temperature decreasing to the Curie temperature $T_C \sim 23$ K. The magnetic hysteresis loop observed below T_C [e.g., at 2 K shown in the inset of Fig. 2(a)] is also in accordance with the FM ordering. When the linear thermal expansion, defined as $\Delta L/L = [L(T) - L(2\text{K})]/L(2\text{K})$, is measured as a function of temperature at zero field, one finds that the thermal expansion gradually decreases with decreasing temperature in the PM state, indicating the occurrence of normal positive thermal expansion. Unexpectedly, however, the thermal expansion experiences an inflection point at T_C , below which the linear thermal expansion unusually increases on cooling. This indicates that negative thermal expansion takes place in the FM state in the z-type DyCrO₄. This coincidence suggests a strong magnetocrystalline coupling. A detailed description of the z-type structure is reported in Refs. [21,22]. A tetragonal-to-orthorhombic crystal structural phase transition is determined between 40 and 27 K due to pseudo-Jahn–Teller effects, leading to a reduction

in symmetry from *I*4₁/*amd* to *Imma*. A more microscopic perspective is the splitting of the accidental orbital degeneracy or near-degeneracy in crystal field levels,^[24] causing a slight shift of Cr⁵⁺ along the *z*-axis direction, accompanied by an increase in the Cr–O and Dy–O bond lengths. This structural symmetry change and orthogonal distortion of the lattice can be considered as the mechanism of negative thermal expansion presented in the z-type DyCrO₄ at low temperatures. The inflection point of thermal expansion observed near T_C arises from lattice distortion via spin–lattice coupling.

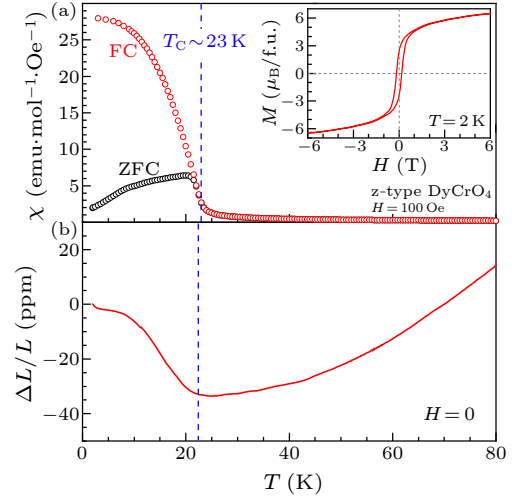


Fig. 2. Magnetic and thermal-expansion properties of the z-type DyCrO₄. (a) Temperature dependence of zero-field-cooling (ZFC) and field-cooling (FC) magnetic susceptibility measured at 100 Oe. The inset shows the isothermal magnetization measured at 2 K. (b) Temperature dependence of linear thermal expansion. The dashed line indicates the FM phase transition and thermal expansion variation at T_C .

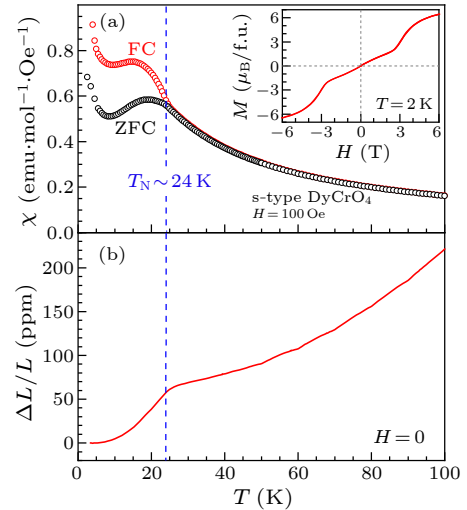


Fig. 3. Magnetic and thermal-expansion properties of the s-type DyCrO₄. (a) Temperature dependence of ZFC and FC magnetic susceptibility measured at 100 Oe. The inset shows the isothermal magnetization measured at 2 K. (b) Temperature dependence of linear thermal expansion. The dashed line indicates the antiferromagnetic (AFM) phase transition and thermal expansion anomaly at T_N .

Similarly, temperature-dependent susceptibility and linear thermal expansion were measured for the s-type DyCrO₄. In contrast to the FM phase transition observed in the z-type phase, the s-type phase undergoes an AFM transition on cooling to the Néel temperature $T_N \sim 24$ K, as presented in Fig. 3(a). The T_N is determined based on the onset of separation between the zero-field-cooling (ZFC) and field-cooling (FC) susceptibility curves, in agreement with the anomaly occurring in specific heat.^[25] Moreover, a field-induced metamagnetic transition from the initial collinear AFM structure to a canted AFM state with considerable net FM moment is found to occur as the field increases to approximately 3 T [see the inset of Fig. 3(a)], which is consistent with the previous reports.^[26] Although negative thermal expansion is observed at the FM state of the z-type phase, the s-type DyCrO₄, at zero field, displays only positive thermal expansion in both the PM and AFM states. However, a remarkable anomaly appears near T_N , below which the thermal expansion sharply decreases with further cooling. This spontaneous change in dimensions at T_N is also indicative of a strong magneto-structural correlation in the s-type phase, similar to that in the z-type one. Note that no structural phase transition occurs in the s-type phase at temperatures down to 2 K, so the positive thermal expansion remains across the whole temperature region measured (3–50 K) at zero field.

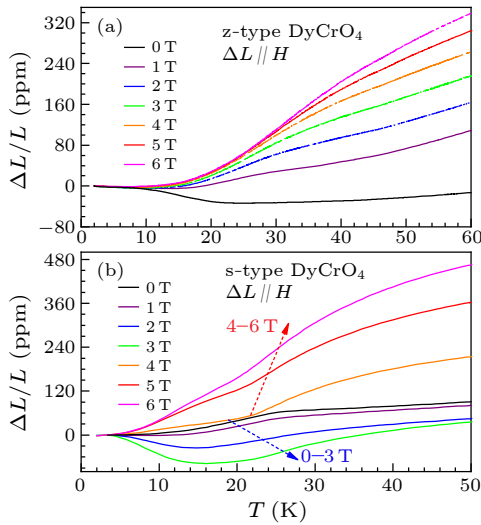


Fig. 4. Thermal expansion measured at different magnetic fields. Temperature dependence of linear thermal expansion of (a) z-type and (b) s-type DyCrO₄ in a series of magnetic fields applied along the direction of sample length. The arrows in (b) indicate the tendency of thermal expansion with increasing magnetic field.

As strong magnetocrystalline coupling is present in both the z- and s-type DyCrO₄, it is intriguing to study the magnetic field effects on the thermal expansion of these two phases. Figure 4(a) shows the temperature dependence of linear thermal expansion measured at selected fields for the z-type phase. One finds that the thermal expansion is highly sensitive to external magnetic fields. Specifically,

the normal positive thermal expansion above T_C is considerably enhanced with increasing magnetic field. The change in thermal expansion is as large as 300 ppm between 0 and 6 T at 50 K. More interestingly, the negative thermal expansion below T_C is greatly suppressed once a magnetic field is applied. More specifically, the z-type phase has a pronounced negative thermal expansion with an average linear CTE of $\bar{\alpha}_L = -1.59$ ppm·K⁻¹ at 3–23 K without applying a magnetic field (i.e., at $H = 0$ T). Here, $\bar{\alpha}_L$ is calculated using the function $\bar{\alpha}_L = [\Delta L/L]/\Delta T$. As the magnetic field is applied to 1 T, the negative thermal expansion changes to a near-zero thermal expansion with a value of $\bar{\alpha}_L = 0.59$ ppm·K⁻¹ at 3–23 K. Note that this magnitude of $\bar{\alpha}_L$ for the z-type DyCrO₄ is even less than that of the commercial zero-thermal-expansion material of invar alloys (1.2 ppm·K⁻¹ at 300 K).^[1] Above 1 T, the thermal expansion becomes completely positive across the whole temperature range regardless of the FM state.

Compared with the z-type phase, the s-type phase of DyCrO₄ exhibits more complex thermal expansion behavior under external magnetic fields. As shown in Fig. 4(b), as magnetic fields are gradually applied from 0 to 3 T, the magnitude of thermal expansion is reduced as a whole over the temperature range of 3–50 K. In particular, at lower temperatures, the initially positive thermal expansion is induced into negative. Moreover, the amplitude of negative thermal expansion increases with increasing magnetic field. For instance, the calculated value of $\bar{\alpha}_L$ changes from positive 2.69 ppm·K⁻¹ at 0 T to -2.7 ppm·K⁻¹ at 3 T in the temperature region of 3–24 K (i.e., below T_N). However, once the magnetic field increases above 3 T, which is the critical field for the metamagnetic transition, the whole magnitude of thermal expansion is sharply enhanced, and the sign of $\bar{\alpha}_L$ is also switched from negative to positive again. The negative thermal expansion induced at lower magnetic fields in the s-type DyCrO₄ looks similar to the zero-field behavior observed in the z-type phase, as both can be tuned positive by higher fields.

Figures 5(a) and 5(b) summarize the average linear CTE of $\bar{\alpha}_L$ as a function of magnetic field for the z-type DyCrO₄ in 3–23 K and the s-type phase in 3–24 K, respectively, i.e., in the spin-ordering states for these two phases. For the z-type phase, a small field close to 1 T can tune the sign change of thermal expansion from negative to positive. Moreover, the magnitude of $\bar{\alpha}_L$ tends to saturation with increasing field above 4 T. Based on previous neutron diffraction data,^[22] the tetragonal z-type DyCrO₄ changes into an orthorhombic phase, where both a and c axes slightly expand on cooling from 27 to 3.6 K, whereas tiny contraction occurs for b axis. We therefore infer that the negative thermal expansion is caused by a and c axes. In comparison, the s-type phase also exhibits very sensitive field dependence. A moderate field near 2 T can induce the initially positive thermal expansion to be negative. The negative thermal expansion is still field variable, and a higher field up to approximately 3.5 T can change the sign again. Therefore, magnetic-field-induced sign changes of thermal expansion from positive to negative and then to reentrant positive are realized in

the s-type DyCrO₄. According to our neutron diffraction study of the s-type DyCrO₄ as a function of magnetic field, the intensity of the magnetic (002) reflection peak gradually decreases with the increasing magnetic field.^[26] This indicates that the magnetic moments rotate toward the applied magnetic field, inducing canting of the collinear AFM structure, which yields a net FM moment. The competing of the coexisting magnetic states of collinear AFM and FM structures under magnetic field could result in an unusual thermal expansion transformation as a function of magnetic field.^[27] Similar phenomena could also be expected in the z-type DyCrO₄. Note that such a series of field-induced sign changes in thermal expansion have never been found in other material systems. The present study sheds light on the potential of external magnetic field as an effective method to control thermal expansion, including the magnitude and sign, via strong magnetocrystalline coupling.

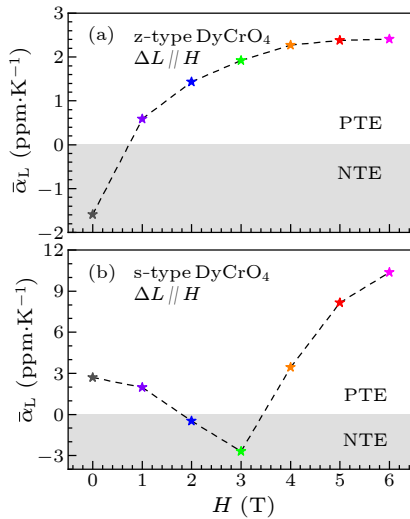


Fig. 5. Coefficient of average linear thermal expansion at different magnetic fields. Average linear coefficient of thermal expansion of (a) z-type at 3–23 K and (b) s-type DyCrO₄ at 3–24 K in a series of magnetic fields applied along the direction of sample length. PTE: positive thermal expansion, NTE: negative thermal expansion.

We then studied the magnetostrictive effects by scanning the field strength from 10 to -10 T at selected temperatures for DyCrO₄. As shown in Fig. 6(a), the absolute magnetostriction of the z-type phase increases with decreasing temperature and reaches 860 ppm at 2 K and 10 T, indicating a large spin–lattice coupling, which may be derived from the larger magnetic moment of Dy³⁺. Such a significant magnetostrictive effect of DyCrO₄ is larger than those of familiar rare-earth intermetallic compounds, such as Fe–Ga alloys and DyNi₂,^[28,29] and some rare-earth-based antiferromagnets, such as DyNi₂B₂C.^[30] Moreover, the magnetostriction of the z-type DyCrO₄ shows no trace of saturation even at field strengths up to 10 T. The value of magnetostriction is expected to be greater in a higher external magnetic field. In rare-earth metals, alloys, and intermetallic compounds, the giant magnetostrictive effect is mainly caused by the unfilled 4*f* layer electrons.^[31] The 4*f*

electron orbitals of rare-earth ions have strong anisotropy. When spontaneously magnetized, the 4*f* layer electrons achieve the lowest energy in one or more specific directions. This causes large lattice distortion along these directions, resulting in giant magnetostriction. According to previous studies, both the Cr⁵⁺ and Dy³⁺ spin moments collinearly align along the *y*-axis direction in the z-type DyCrO₄. Therefore, the magnetic interactions between Cr⁵⁺ and Dy³⁺ ions should be mainly responsible for the FM transition of DyCrO₄, as Buisson *et al.* reported for the FM origin of the isostructural TbCrO₄ system.^[32] There is large strain-dependent anisotropy of the rare-earth ion Dy³⁺ situated at the centers of the dodecahedrons and Cr⁵⁺ at the centers of the tetrahedra in the lattice. With increasing magnetic field, the spins of Dy³⁺ and Cr⁵⁺ ions rotate under the action of the external field. The lattice size of the sample is then affected by the spin–lattice coupling interaction, and the macroscopically manifested magnetostrictive behavior is that the lattice shrinks with increasing magnetic field at fixed temperatures.

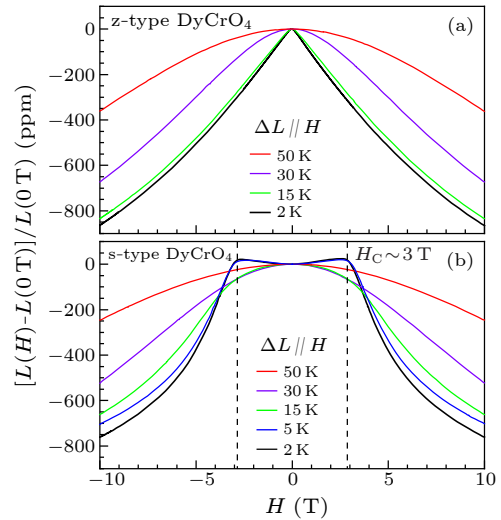


Fig. 6. Field dependence of magnetostriction for (a) z-type and (b) s-type DyCrO₄ at selected temperatures.

In sharp contrast to the monotonic magnetostrictive feature observed in the z-type phase, the magnetostriction of the s-type DyCrO₄ at low temperatures (i.e., 2 and 5 K) exhibits a sign change from positive to negative at a critical field strength of approximately 3 T, as presented in Fig. 6(b). This critical magnetic field is just in line with the metamagnetic transformation from the collinear AFM to a canted one with considerable net FM moment [see the inset of Fig. 3(a)]. Above the critical field, the absolute magnetostriction also increases with decreasing temperature and reaches 760 ppm in 10 T at 2 K. The sign change of the magnetostriction curve in the s-type DyCrO₄ implies that there are two competing factors affecting magneto-lattice coupling under the influence of a magnetic field. According to the neutron diffraction data, at zero magnetic field, the spin structure composed of Cr⁵⁺ and Dy³⁺ is collinear AFM with spin moments parallel to the *c*-axis of the crystal lattice. Magnetic symmetry analysis illustrates that the collinear AFM structure of the s-type DyCrO₄

has a magnetic point group of $2'/m$, with two-fold rotation along the c -axis, whereas the mirror is perpendicular to the c -axis.^[21] The magnetic anisotropies of Dy^{3+} and Cr^{5+} are opposite in direction. When a magnetic field is applied to the AFM phase, the AFM interactions of the Dy^{3+} and Cr^{5+} ions in the lattice are enhanced. However, this stress cannot be released by the rotation of the spin directions. Under the spin–lattice interaction, the lattice is forced to expand to release stress potential energy. When the magnetic field exceeds 3 T, the sample is in a canted AFM state, retaining a net magnetic moment in the easy axis direction, similar to the FM state in the z -type phase. The strong anisotropy of $4f$ layer electrons, magnetic anisotropy of Dy^{3+} and Cr^{5+} , coupled with spin–lattice interactions can rationally explain the characteristics of notable magnetostriction and sign changes of thermal expansion under different magnetic fields. In addition to the mechanisms mentioned above, the magnetostriction in a magnetic crystal under an applied magnetic field can be due to the movement of twin boundaries and the alignment of FM or AFM domains.^[33,34] Moreover, the magnetostriction of DyCrO_4 polycrystal can be affected by grain orientations and magnetic domain configurations.^[35]

In summary, we have demonstrated significant magnetic field effects on the thermal expansion and large magnetostriction of polycrystalline z - and s -type DyCrO_4 samples prepared under ambient and high-pressure conditions, respectively. The z -type phase exhibits a negative CTE below the FM-order temperature of 23 K at zero field. The sign of the CTE changes from negative to positive with increasing magnetic field up to 1 T. The induced positive CTE appears to saturate above 4 T. In the s -type phase, the magnetic field can change the initially positive CTE to be negative with a field strength of up to 2.0 T below the AFM-order temperature of 24 K. Furthermore, the negative CTE reenters into positive by enhancing the field ≥ 3.5 T. Both the z - and s -type phases exhibit large magnetostriction with the absolute values up to ~ 800 ppm at 2 K and 10 T. The physical origins of the tunable negative thermal expansion and the large magnetostriction are closely related to the strong spin–lattice coupling. The present study provides an unprecedented example of external magnetic fields significantly changing the thermal expansion, including the magnitude and especially the sign, which opens up a new avenue in readily controlling thermal expansion.

Methods. The polycrystalline z -type DyCrO_4 samples were prepared using stoichiometric ratios of $\text{Dy}(\text{NO}_3)_3 \cdot 6\text{H}_2\text{O}$ and $\text{Cr}(\text{NO}_3)_3 \cdot 9\text{H}_2\text{O}$ as starting materials. A similar heat-treatment process to that reported in Ref. [36] was used at ambient pressure. The green z -type DyCrO_4 was then adopted as a precursor material. After treating the precursor at 3.0 GPa and 850 K for 15 min on a cubic anvil-type high-pressure apparatus, black s -type DyCrO_4 samples were obtained. To identify the sample quality and determine the crystal structures of these two products, powder XRD measurement was performed at room temperature using a Huber diffractometer with $\text{Cu } K_{\alpha 1}$ radiation in a 2θ range from 10° to 100° with steps

of 0.005° . Rietveld refinement of the XRD data was performed using the GSAS program.^[37]

The temperature dependence of magnetic susceptibility and field-dependent isothermal magnetization were measured on a magnetic property measurement system (Quantum Design, MPMS XL-7). Both ZFC and FC modes were used for susceptibility measurements at a magnetic field of 100 Oe. A home-made capacitance dilatometer was used to measure the thermal expansion and magnetostriction in a cryogen-free superconducting magnet system (Oxford Instruments, TeslatronPT), as described in detail elsewhere.^[38,39] Rod-shaped specimens of 3.196 mm length and 2.4 mm diameter for the z -type DyCrO_4 , and 2.771 mm length and 2.1 mm diameter for the s -type phase, were used for these measurements. The samples were clamped between the upper parallel plate and the supporting structure of the dilatometer. As the temperature and/or magnetic field change, the sample is deformed, which induces movement of the upper parallel plate, so that the capacitance of the parallel plates changes. Using an AH2700 capacitance bridge to precisely measure the capacitance, the deformation of the sample can be deduced at a high accuracy of 10^{-9} – 10^{-10} m by the following formula:

$$\Delta L = -\varepsilon_0 \pi r^2 \left(\frac{C_1 - C_2}{C_1 C_2} - \frac{C_1 - C_2}{C_{\max}^2} \right). \quad (1)$$

Here, ΔL is the change of sample length along the measurement direction, ε_0 is the vacuum dielectric constant, r is the radius of the capacitor plate, C_1 and C_2 are the changing capacitance and the initial capacitance value, respectively. C_{\max} is called the short-circuit capacitance, which is the maximum capacitance measured by carefully decreasing the plate distance with the adjustment screw until the capacitor is under short-circuit condition. During the thermal expansion measurements, the sample was cooled from 50 K to 3 K at different applied magnetic fields, and then the thermal expansion was measured by slowly heating the sample with the applied magnetic field. The heating rate was 1 K/min. The magnetostriction measurements were carried out by keeping the samples at a fixed temperature and then slowly changing the applied magnetic field in the range from -10 T to 10 T at a rate of 10 Oe/s.

Acknowledgements. This work was supported by the National Key R&D Program of China (Grant Nos. 2021YFA1400300 and 2018YFA0305700), the National Natural Science Foundation of China (Grant Nos. 11934017, 12261131499, 51725104, 11921004, 11904392, and 22271309), the Beijing Natural Science Foundation (Grant No. Z200007), and the Chinese Academy of Sciences (Grant No. XDB33000000).

References

- [1] Chen J, Hu L, Deng J, and Xing X 2015 *Chem. Soc. Rev.* **44** 3522
- [2] Takenaka K 2012 *Sci. Technol. Adv. Mater.* **13** 13001
- [3] Venkataraman G, Feldkamp L A, and Sahn V C 1975 *Dynamics of Perfect Crystals* (Cambridge: MIT Press)

- [4] Chen J *et al.* 2013 *Sci. Rep.* **3** 2458
- [5] Mary T A, Evans J S O, Vogt T, and Sleight A W 1996 *Science* **272** 90
- [6] Greve B K *et al.* 2010 *J. Am. Chem. Soc.* **132** 15496
- [7] Goodwin A L *et al.* 2008 *Science* **319** 794
- [8] Takenaka K and Takagi H 2005 *Appl. Phys. Lett.* **87** 261902
- [9] van Schilfgaarde M, Abrikosov I A, and Johansson B 1999 *Nature* **400** 46
- [10] Yu C Y *et al.* 2021 *Nat. Commun.* **12** 4701
- [11] Takenaka K, Okamoto Y, Shinoda T, Katayama N, and Sakai Y 2017 *Nat. Commun.* **8** 14102
- [12] Long Y W *et al.* 2009 *Nature* **458** 60
- [13] Azuma M *et al.* 2011 *Nat. Commun.* **2** 347
- [14] Asai D *et al.* 2019 *Appl. Phys. Lett.* **114** 141902
- [15] Chen J *et al.* 2011 *J. Am. Chem. Soc.* **133** 11114
- [16] Pan Z *et al.* 2017 *J. Am. Chem. Soc.* **139** 14865
- [17] Ren Z H *et al.* 2018 *Nat. Commun.* **9** 1638
- [18] Kou R H *et al.* 2016 *J. Mater. Sci.* **51** 1896
- [19] Song Y Z *et al.* 2020 *Chem. Mater.* **32** 7535
- [20] Long Y W *et al.* 2008 *J. Appl. Phys.* **103** 93542
- [21] Midya A, Khan N, Bhoi D, and Mandal P 2013 *Appl. Phys. Lett.* **103** 92402
- [22] Long Y W *et al.* 2010 *J. Magn. Magn. Mater.* **322** 1912
- [23] Smirnov M B, Mirgorodsky A P, Kazimirov V Y, and Guinebretière R 2008 *Phys. Rev. B* **78** 94109
- [24] Gehring G A and Gehring K A 1975 *Rep. Prog. Phys.* **38** 1
- [25] Long Y W, Liu Q Q, Lv Y X, Yu R C, and Jin C Q 2011 *Phys. Rev. B* **83** 024416
- [26] Shen X D *et al.* 2019 *NPG Asia Mater.* **11** 50
- [27] Kobayashi M and Mochizuki M 2019 *Phys. Rev. Mater.* **3** 024407
- [28] Xing Q, Du Y, McQueeney R J, and Lograsso T A 2008 *Acta Mater.* **56** 4536
- [29] Ibarra M R and Moral A D 1990 *J. Magn. Magn. Mater.* **83** 121
- [30] Sierks C *et al.* 1999 *J. Magn. Magn. Mater.* **192** 473
- [31] Cullen J R and Clark A E 1977 *Phys. Rev. B* **15** 4510
- [32] Buisson G, Tchéou F, Sayetat F, and Scheunemann K 1976 *Solid State Commun.* **18** 871
- [33] Alberts L and Lee E W 1961 *Proc. Phys. Soc.* **78** 728
- [34] He A N, Ma T Y, Zhang J J, Luo W, and Yan M 2009 *J. Magn. Magn. Mater.* **321** 3778
- [35] Peng W Y and Zhang J H 2006 *Appl. Phys. Lett.* **89** 262501
- [36] Long Y W 2007 *Phys. Rev. B* **75** 104402
- [37] Toby B H and Von Dreele R B 2013 *J. Appl. Crystallogr.* **46** 544
- [38] Ma Y N, Wang Y X, Cong J C, and Sun Y 2019 *Phys. Rev. Lett.* **122** 255701
- [39] Chai Y S, Cong J Z, He J C, Su D, Ding X X, Singleton J, Zapf V, and Sun Y 2021 *Phys. Rev. B* **103** 174433

Supplementary Material: Magnetic-Field-Induced Sign Changes of Thermal Expansion in DyCrO₄

Jin-Cheng He(何金城)^{1,2#}, Zhao Pan(潘昭)^{1,2#}, Dan Su(苏丹)^{1,2}, Xu-Dong Shen(申旭东)^{1,2}, Jie Zhang(张杰)^{1,2}, Da-Biao Lu(卢达标)^{1,2}, Hao-Ting Zhao(赵浩婷)^{1,2}, Jun-Zhuang Cong(丛君状)¹, En-Ke Liu(刘恩克)^{1,2}, You-Wen Long(龙有文)^{1,2,3**}, and Young Sun(孙阳)^{1,4**}

¹Beijing National Laboratory for Condensed Matter Physics, Institute of Physics, Chinese Academy of Sciences, Beijing 100190, China

²School of Physical Sciences, University of Chinese Academy of Sciences, Beijing 100190, China

³Songshan Lake Materials Laboratory, Dongguan, Guangdong 523808, China

⁴Center of Quantum Materials and Devices, and Department of Applied Physics, Chongqing University, Chongqing 401331, China

Table S1. Refined structural parameters of the zircon- and scheelite-type DyCrO₄ at room temperature.

Composition	Space group	Atom	Site	g	x	y	z	100×U _{iso} (Å ²)
<i>z</i> -DyCrO ₄ ^a	<i>I</i> 4 ₁ / <i>amd</i>	Dy	4a	1	0	0.75	0.125	2.5
		Cr	4b	1	0	0.25	0.375	2.5
		O	16h	1	0	0.4299	0.2021	2.5
<i>s</i> -DyCrO ₄ ^b	<i>I</i> 4 ₁ / <i>a</i>	Dy	4b	1	0	0.25	0.625	2.5
		Cr	4a	1	0	0.25	0.125	2.5
		O	16f	1	0.2534(6)	0.1058(4)	0.0475(1)	2.5

^aSpace group: *I*4₁/*amd*, $a = b = 7.13742(7)$ Å, $c = 6.26562(7)$ Å, $V = 319.188(9)$ Å³, $\alpha = \beta = \gamma = 90^\circ$. *R*-factor: $R_{wp} = 6.65\%$, $R_p = 4.62\%$.

^bSpace group: *I*4₁/*a*, $a = b = 5.015(5)$ Å, $c = 11.310(9)$ Å, $V = 284.531(9)$ Å³, $\alpha = \beta = \gamma = 90^\circ$.

R-factor: $R_{wp} = 2.3\%$, $R_p = 1.73\%$.